

The British University in Egypt

**BUE Scholar**

---

Centre for Advanced Materials

Research Centres

---

2010

## **Multiscale transformation field analysis of progressive damage in fibrous laminates**

Yehia Bahei-El-Din

Ritesh Khire

Prabhat Hajela

Follow this and additional works at: [https://buescholar.bue.edu.eg/centre\\_advanced\\_materials](https://buescholar.bue.edu.eg/centre_advanced_materials)



Part of the [Computational Engineering Commons](#), [Engineering Mechanics Commons](#), [Mechanics of Materials Commons](#), [Structural Materials Commons](#), and the [Structures and Materials Commons](#)

---

# Multiscale Transformation Field Analysis of Progressive Damage in Fibrous Laminates

Yehia A. Bahei-El-Din  
*Centre for Advanced Materials  
The British University in Egypt  
El-Shorouk City, Egypt*

Ritesh Khire and Prabhat Hajela  
*Department of Mechanical, Aerospace and Nuclear Engineering  
Rensselaer Polytechnic Institute, Troy, NY 12180, USA*

As part of an ongoing effort to model uncertainty propagation across multiple scales in fibrous laminates, this paper presents a deterministic transformation field analysis for modeling damage progression under membrane forces and bending moments. In this approach, equivalent eigenstresses are computed in the phases and/or plies such that their respective stress components which satisfy the underlying failure criteria are reduced to zero. Superposition of the solutions found for fiber the undamaged laminate under applied loads and under the eigenstress field provide the entire response. Failure criteria are based on stress averages in the and matrix. Damage mechanisms considered are frictional sliding and splitting on matrix planes which are parallel to the fiber direction, and fiber breakage. Model predictions correlate well with published experimental measurements for the stress-strain response as well as failure envelope.

## Nomenclature

$A_r$	=	strain concentration factors of a phase
$B_r$	=	stress concentration factors of a phase
$D_{rs}$	=	strain influence functions of a phase
$E$	=	Young's modulus
$G$	=	Shear Modulus
$F_{rs}$	=	stress influence functions of a phase
$I$	=	identity matrix
$L$	=	elastic stiffness matrix
$M$	=	elastic compliance matrix
$\mathcal{M}$	=	bending moment
$\mathcal{N}$	=	membrane forces
$N_i$	=	strain transformation matrix of a lamina
$P_i$	=	stress concentration factor matrix of a lamina due to force
$Q_i$	=	stress concentration factor matrix of a lamina due to moment
$R_i$	=	stress transformation matrix of a lamina
$U_{ij}$	=	stress influence functions of a lamina
$c$	=	lamina volume fraction
$h$	=	laminate thickness
$n$	=	number of plies
$t$	=	lamina thickness
$v$	=	phase volume fraction

$\delta_{ij}$	=	Kronecker's delta
$\boldsymbol{\varepsilon}$	=	strain
$\eta$	=	coefficient of friction
$\boldsymbol{\kappa}$	=	curvature
$\boldsymbol{\lambda}$	=	eigenstress
$\boldsymbol{\mu}$	=	eigenstrain
$\nu$	=	Poisson's ratio
$\boldsymbol{\sigma}$	=	stress
$\sigma_u$	=	ultimate normal strength
$\tau_u$	=	ultimate shear strength
$\varphi$	=	fiber orientation angle

## I. Introduction

THE inclusion of uncertainty and risk in the simulation-based optimal design of structural composites requires an integrated approach which models these effects in mechanistic models of deformation and damage. To depart from deterministic design approaches in which the mechanistic models are linked to formal mathematical methods of optimization, multiscale probabilistic models that yield a hierarchical description of initiation and propagation of damage as well as inelastic deformations in composite structural systems are presently pursued<sup>1,2</sup>.

An essential element of this approach is a computationally tractable formulation of the composite analysis problem that takes into consideration the inherent multiscale nature of the problem. The modeling of failure in composite materials however often treats the material as macroscopically homogeneous and examines overall failure criteria without reference to progression of damage. This is primarily due to the lack of mathematical models, which link the overall response to the local phenomena, despite the extensive information available for the latter including experiments and constitutive theories.

Attempts to relate local damage to the overall behavior of composite materials and to structural components by mathematical and/or computational models are few, and relatively new. A class of models in this direction centers on the transformation field analysis (TFA) approach, which evaluates interactions between the various deformation and damage mechanisms in composite or polycrystalline aggregates. Originally developed and implemented in analysis of composites with viscoelastic, viscoplastic and elastic-plastic phases<sup>3,4,5</sup>, the method has seen recently direct applications to describe damage events such as reinforcement debonding in two phase composites<sup>6</sup>, fiber debonding and sliding in fibrous composites<sup>7,8</sup> and in laminates<sup>9</sup>, and internal damage modes in woven composites<sup>10</sup>, as well as utilization in homogenization techniques<sup>11,12,13,14</sup>. In principle, the method evaluates interaction of applied

and residual stress and strain fields caused by distributions of eigenstrains in heterogeneous solids. Regardless of their origin, the TFA regards such transformation strains as distributed internal loads that act on an otherwise undamaged elastic composite aggregate.

This paper develops a TFA approach for fibrous laminates of a general layup under membrane forces and bending moments as well as local eigenstress fields. The latter is introduced to model the effect of damage in the fiber and matrix on the strain and curvature of the laminate. Mechanical behavior of unidirectional plies was modeled with a two-phase, averaging material model, and the laminate deformations were assumed to follow the Kirchhoff idealization. The paper is organized as follows; Section II describes geometry, material and load. Micromechanics of a unidirectional fibrous lamina is described in Section III, and macromechanics of laminates is given in Section IV. The TFA approach is developed in Section V followed by description of the failure criteria in Section VI. Results, which compare the model predictions with experimental measurements, are given in Section VII. The paper concludes with a closure in Section VIII, which summarizes the work performed and discusses related issues that can benefit from future research.

The notation used here are symbolic, where symmetric second-order tensors are written as (6x1) matrices and denoted by boldface, lower case letters, and symmetric fourth-order tensors are written as (6x6) matrices and denoted by boldface, upper case letters. Connections with tensor notation are easily established. For example, the stress tensor  $\sigma_{ij}$ , and strain tensor  $\varepsilon_{ij}$ , with the symmetry  $\sigma_{ij} = \sigma_{ji}$ ,  $\varepsilon_{ij} = \varepsilon_{ji}$ , are written in matrix form as  $\boldsymbol{\sigma} = [\sigma_{11}, \sigma_{22}, \sigma_{33}, \sigma_{23}, \sigma_{31}, \sigma_{12}]$ , and  $\boldsymbol{\varepsilon} = [\varepsilon_{11}, \varepsilon_{22}, \varepsilon_{33}, 2\varepsilon_{23}, 2\varepsilon_{31}, 2\varepsilon_{12}]$ . Similarly, fourth-order tensors having at least the symmetries  $A_{ijkl} = A_{jikl} = A_{ijlk}$  are reduced to (6x6) matrices  $\mathbf{A}$ , such that  $\mathbf{A}\mathbf{A}^{-1} = \mathbf{A}^{-1}\mathbf{A} = \mathbf{I}$ , the identity matrix.

## II. Geometry, Material and Load

The fibrous laminate under consideration consists of  $N$  fully bonded thin elastic plies, Fig. 1. The ply thickness is denoted  $t_i$ ,  $i = 1, 2, \dots, n$ , such that  $\sum t_i = h$ , the total thickness of the laminate. Hence,  $c_i = t_i / h$  is the volume fraction of ply ‘ $i$ ’, such that  $\sum c_i = 1$ . Two coordinate systems are defined as shown in Fig. 1, one is overall ( $x_j$ ,  $j = 1, 2, 3$ ), and one is local ( $\bar{x}_k$ ,  $k = 1, 2, 3$ ). The latter coincides with material principal axes of a unidirectional composite lamina. Fiber orientation of ply ‘ $i$ ’ is given by angle  $\varphi_i$  between the local  $\bar{x}_1$  and the overall  $x_1$  axes.

Both membrane forces,  $\mathcal{N} = [\mathcal{N}_1, \mathcal{N}_2, \mathcal{N}_{12}]$ , and bending moments,  $\mathcal{M} = [\mathcal{M}_1, \mathcal{M}_2, \mathcal{M}_{12}]$ , are considered. Let  $\hat{\boldsymbol{\sigma}}(z) = [\hat{\sigma}_{11}, \hat{\sigma}_{22}, \hat{\sigma}_{12}]$  denote in-plane stresses caused in the laminate, where  $z \equiv x_3$  denote the distance across the laminate thickness, measured from the geometric mid-plane  $x_1x_2$ , Fig. 1. Hence,

$$\mathcal{N} = \int_{-h/2}^{h/2} \hat{\boldsymbol{\sigma}}(z) dz = \sum_{i=1}^n \left( \int_{z_i - t_i/2}^{z_i + t_i/2} \hat{\boldsymbol{\sigma}}(z) dz \right), \quad (1)$$

$$\mathcal{M} = \int_{-h/2}^{h/2} z \hat{\boldsymbol{\sigma}}(z) dz = \sum_{i=1}^n \left( \int_{z_i - t_i/2}^{z_i + t_i/2} z \hat{\boldsymbol{\sigma}}(z) dz \right), \quad (2)$$

where  $z_i$  is the  $x_3$  coordinate of the mid plane of lamina ‘ $i$ ’.

Properties of the unidirectionally reinforced plies are given in terms of elastic moduli of the fiber ( $f$ ) and matrix ( $m$ ) materials, and their volume fractions,  $v_f, v_m$ , where  $v_f + v_m = 1$ . The matrix is assumed to be isotropic with Young’s modulus  $E_m$  and Poisson’s ratio  $\nu_m$ . The fiber is transversely isotropic with  $\bar{x}_1$  as the axis of rotational symmetry,  $E_L^f$  and  $E_T^f$  the longitudinal and transverse Young’s moduli,  $\nu_L^f$  and  $\nu_T^f$  the associated Poisson’s ratios, and  $G_L^f$  the longitudinal shear modulus. Consequently, the unidirectional plies are transversely isotropic with overall elastic properties analogous to those of the fiber;  $E_L, E_T, \nu_L, \nu_T, G_L$ . The overall properties can be either measured or computed from the local properties using a micromechanical model<sup>15</sup>. When certain fiber properties are difficult to measure, they can be back calculated from a material model and the measured overall properties as well as those of the matrix<sup>16</sup>.

### III. Ply Micromechanics

Consider a two phase composite with known fiber and matrix elastic properties and volume fractions as detailed above. The local stresses and strains vary pointwise but will be approximated by the average fields in the fiber and matrix. Let  $\boldsymbol{\sigma}_r$  and  $\boldsymbol{\varepsilon}_r$ ,  $r = f, m$ , denote the stress and strain averages in the fiber and matrix, and  $\bar{\boldsymbol{\sigma}}$  and  $\bar{\boldsymbol{\varepsilon}}$  denote uniform overall stresses and strains. In general, these stress and strain vectors contain six independent components. The reference coordinate system for both the local and overall fields of a unidirectional composite is the material principal axes  $\bar{x}_k$ ,  $k = 1, 2, 3$ , Fig. 1. The local and overall fields are related by

$$\bar{\sigma} = v_f \sigma_f + v_m \sigma_m, \quad \bar{\varepsilon} = v_f \varepsilon_f + v_m \varepsilon_m. \quad (3)$$

Constitutive equations of the phases subjected to  $\varepsilon_r$ , or  $\sigma_r$ , and simultaneously supporting uniform transformation, or eigen, stress  $\lambda_r$ , or strain  $\mu_r$ , are written as

$$\sigma_r = L_r \varepsilon_r + \lambda_r, \quad \varepsilon_r = M_r \sigma_r + \mu_r, \quad (4)$$

where  $L_r$  and  $M_r = L_r^{-1}$  are elastic stiffness and compliance. The transformation stress and strain are related by  $\lambda_r = -L_r \mu_r$ , and represent fields that are either intrinsic and cannot be recovered by mechanical unloading such as thermal and plastic strain, or introduced as auxiliary fields.

Similarly, constitutive equations for a composite lamina subjected to overall uniform strain  $\bar{\varepsilon}$ , or stress  $\bar{\sigma}$ , and uniform transformation stress  $\bar{\lambda}$ , or strain  $\bar{\mu}$ , are written in the material principal axes  $\bar{x}_k$  as

$$\bar{\sigma} = \bar{L} \bar{\varepsilon} + \bar{\lambda}, \quad \bar{\varepsilon} = \bar{M} \bar{\sigma} + \bar{\mu}, \quad (5)$$

where  $\bar{L}$  and  $\bar{M} = \bar{L}^{-1}$  are overall elastic stiffness and compliance, and  $\bar{\lambda} = -\bar{L} \bar{\mu}$ .

The connection between the local strain and stress fields and their overall counterparts are found by superposition of mechanical and transformation field contributions<sup>3</sup>,

$$\varepsilon_r = A_r \bar{\varepsilon} + \sum_{s=f,m} D_{rs} \mu_s, \quad \sigma_r = B_r \bar{\sigma} + \sum_{s=f,m} F_{rs} \lambda_s, \quad r = f, m. \quad (6)$$

Here,  $A_r$  and  $B_r$  represent strain and stress concentration factors for the fiber and matrix<sup>17,18</sup>, and  $D_{rs}$  and  $F_{rs}$  are transformation influence functions. Both the concentration factors and the transformation influence functions depend on mutual constraints of the phases and their elastic moduli. Closed forms for the concentration factors and influence functions can be found for two-phase models of fibrous composites<sup>17,19</sup>.

If the concentration factors  $A_r$  and  $B_r$  are known, one can find from Eqs. (3)-(6), in the absence of transformation fields, the overall elastic stiffness and compliance in the form

$$\bar{L} = v_f L_f A_f + v_m L_m A_m, \quad \bar{M} = v_f M_f B_f + v_m M_m B_m. \quad (7)$$

The overall transformation stress and strain are given in terms of their local counterparts by the generalized Levin's<sup>20</sup> formula<sup>4</sup>,

$$\bar{\boldsymbol{\lambda}} = \nu_f \mathbf{A}_f^T \boldsymbol{\lambda}_f + \nu_m \mathbf{A}_m^T \boldsymbol{\lambda}_m, \quad \bar{\boldsymbol{\mu}} = \nu_f \mathbf{B}_f^T \boldsymbol{\mu}_f + \nu_m \mathbf{B}_m^T \boldsymbol{\mu}_m. \quad (8)$$

If only in-plane stresses are of interest, the stress-strain relations (5) assume the following form

$$\hat{\boldsymbol{\sigma}} = \hat{\mathbf{L}} \hat{\boldsymbol{\varepsilon}} + \hat{\boldsymbol{\lambda}}, \quad \hat{\boldsymbol{\varepsilon}} = \hat{\mathbf{M}} \hat{\boldsymbol{\sigma}} + \hat{\boldsymbol{\mu}}, \quad (9)$$

where symbols decorated with a top hat (^) indicate quantities associated with in-plane loads, such that  $\hat{\boldsymbol{\sigma}} = [\bar{\sigma}_{11}, \bar{\sigma}_{22}, \bar{\sigma}_{12}]$  and  $\hat{\boldsymbol{\varepsilon}} = [\bar{\varepsilon}_{11}, \bar{\varepsilon}_{22}, 2\bar{\varepsilon}_{12}]$ . Matrices  $\hat{\mathbf{L}}_i$  and  $\hat{\mathbf{M}}_i = \hat{\mathbf{L}}_i^{-1}$  are stiffness and compliance associated with plane stresses, and  $\hat{\boldsymbol{\mu}}_i$  and  $\hat{\boldsymbol{\lambda}}_i = -\hat{\mathbf{L}}_i \hat{\boldsymbol{\mu}}_i$  are in-plane transformation strain and stress.

The overall stiffness matrix  $\hat{\mathbf{L}}_i$  of a transversely isotropic lamina is given by<sup>21</sup>

$$\hat{\mathbf{L}}_i = \frac{1}{k+m} \begin{bmatrix} E_L k + mn & 2m\ell & 0 \\ 2m\ell & 4km & 0 \\ 0 & 0 & p(k+m) \end{bmatrix} = \hat{\mathbf{M}}_i^{-1}, \quad (10)$$

where  $k, \ell, m, n, p$  are Hill's moduli<sup>22</sup>. They are related to the engineering moduli by  $E_L = n - \ell^2/k$ ,  $\nu_L = \ell/2k$ ,  $m = G_T = E_T/2(1 + \nu_T)$ ,  $p = G_L$ .

When expressed in the overall coordinate system  $x_j$ ,  $j = 1, 2, 3$ , Eq. (9) is written for ply 'i' as

$$\hat{\boldsymbol{\sigma}}_i = \hat{\mathbf{L}}_i \hat{\boldsymbol{\varepsilon}}_i + \hat{\boldsymbol{\lambda}}_i, \quad \hat{\boldsymbol{\varepsilon}}_i = \hat{\mathbf{M}}_i \hat{\boldsymbol{\sigma}}_i + \hat{\boldsymbol{\mu}}_i, \quad (11)$$

where  $\hat{\mathbf{M}}_i = \hat{\mathbf{L}}_i^{-1}$ ,  $\hat{\boldsymbol{\lambda}}_i = -\hat{\mathbf{L}}_i \hat{\boldsymbol{\mu}}_i$ , and<sup>21</sup>

$$\hat{\boldsymbol{\sigma}}_i = \mathbf{R}_i \hat{\boldsymbol{\sigma}}_i, \quad \hat{\boldsymbol{\varepsilon}}_i = \mathbf{N}_i \hat{\boldsymbol{\varepsilon}}_i, \quad (12)$$

$$\hat{\boldsymbol{\lambda}}_i = \mathbf{R}_i \hat{\boldsymbol{\lambda}}_i, \quad \hat{\boldsymbol{\mu}}_i = \mathbf{N}_i \hat{\boldsymbol{\mu}}_i, \quad (13)$$

$$\hat{\mathbf{L}}_i = \mathbf{N}_i^T \hat{\mathbf{L}}_i \mathbf{N}_i, \quad \hat{\mathbf{M}}_i = \mathbf{R}_i^T \hat{\mathbf{M}}_i \mathbf{R}_i, \quad (14)$$

$$\mathbf{R}_i^T = \mathbf{N}_i^{-1} = \begin{bmatrix} \cos^2 \varphi_i & \sin^2 \varphi_i & -\frac{1}{2} \sin 2\varphi_i \\ \sin^2 \varphi_i & \cos^2 \varphi_i & \frac{1}{2} \sin 2\varphi_i \\ \sin 2\varphi_i & -\sin 2\varphi_i & \cos 2\varphi_i \end{bmatrix}, \quad \mathbf{N}_i = \begin{bmatrix} \cos^2 \varphi_i & \sin^2 \varphi_i & \frac{1}{2} \sin 2\varphi_i \\ \sin^2 \varphi_i & \cos^2 \varphi_i & -\frac{1}{2} \sin 2\varphi_i \\ -\sin 2\varphi_i & \sin 2\varphi_i & \cos 2\varphi_i \end{bmatrix}, \quad (15)$$

and  $\varphi_i$  is the angle between the local  $\bar{x}_i$ -axis and the overall  $x_i$ -axis, Fig. 1.

Finally, the in-plane stresses,  $\sigma_{11}$ ,  $\sigma_{22}$ ,  $\sigma_{12}$ , of a ply are identified with the components of the full, six dimensional stress vector using the mapping matrix  $\hat{\mathbf{I}} = (\mathbf{i}_1, \mathbf{i}_2, \mathbf{i}_6)$ , where  $\mathbf{i}_k$  is a column vector of order (6x1) with the  $k^{\text{th}}$  entry equals one, and null entries otherwise. For example, the stresses in ply ‘ $i$ ’ referred to the local coordinate system are written as

$$\bar{\boldsymbol{\sigma}}_i = \hat{\mathbf{I}} \hat{\boldsymbol{\sigma}}_i, \quad \hat{\boldsymbol{\sigma}}_i = \hat{\mathbf{I}}^T \bar{\boldsymbol{\sigma}}_i. \quad (16)$$

Similar equations can be written for the ply stresses referred to the overall coordinate system, and also for the ply eigenstresses.

#### IV. Laminate Macromechanics

We now consider a fibrous laminate with the geometry and load described in Section II. Considering thin laminates, transverse shear deformations are negligible, and the in-plane strains  $\hat{\boldsymbol{\varepsilon}}(z) = [\hat{\varepsilon}_{11}, \hat{\varepsilon}_{22}, 2\hat{\varepsilon}_{12}]$  are assumed to vary linearly across the thickness with the  $x_3 \equiv z$  coordinate. Hence,

$$\hat{\boldsymbol{\varepsilon}}(z) = \boldsymbol{\varepsilon}_o + z\boldsymbol{\kappa}, \quad (17)$$

where  $\boldsymbol{\varepsilon}_o = [\varepsilon_{11}^o, \varepsilon_{22}^o, 2\varepsilon_{12}^o]$  is the strain at the mid-plane of the laminate, and  $\boldsymbol{\kappa} = [\kappa_1, \kappa_2, \kappa_{12}]$  is the curvature with respect to the mid-plane.

Substituting Eq. (9)<sub>1</sub> into Eqs. (1) and (2), and utilizing Eq. (17), the load-response relations for the laminate can be written as

$$\mathcal{N} = \mathbf{A}\boldsymbol{\varepsilon}_o + \mathbf{B}\boldsymbol{\kappa} + \mathbf{f}, \quad \mathcal{M} = \mathbf{B}\boldsymbol{\varepsilon}_o + \mathbf{D}\boldsymbol{\kappa} + \mathbf{g}, \quad (18)$$

where

$$\mathbf{A} = \sum_{i=1}^n t_i \hat{\mathbf{L}}_i, \quad \mathbf{B} = \sum_{i=1}^n (t_i z_i) \hat{\mathbf{L}}_i, \quad \mathbf{D} = \sum_{i=1}^n t_i \left( \frac{1}{12} t_i^2 + z_i^2 \right) \hat{\mathbf{L}}_i, \quad (19)$$

$$\mathbf{f} = \sum_{i=1}^n t_i \boldsymbol{\lambda}_i, \quad \mathbf{g} = \sum_{i=1}^n (t_i z_i) \boldsymbol{\lambda}_i. \quad (20)$$

The first two terms of Eq. (18) are due to mechanical loading. Coupling between membrane and bending deformations is expressed in terms of array  $\mathbf{B}$ , which vanishes for symmetric laminates. Arrays  $\mathbf{f}$  and  $\mathbf{g}$  are eigen-

force and moment caused by eigenstresses present in the plies, such as those developed due to thermal strains, when the laminate is fully constrained.

The inverse relations can be found from Eqs. (18)-(20) as

$$\boldsymbol{\varepsilon}_o = \mathbf{A}'\mathcal{N} + \mathbf{B}'\mathcal{M} + \mathbf{f}', \quad \boldsymbol{\kappa} = \mathbf{C}'\mathcal{N} + \mathbf{D}'\mathcal{M} + \mathbf{g}', \quad (21)$$

where

$$\mathbf{A}' = (\mathbf{I} - \mathbf{B}'\mathbf{B})\mathbf{A}^{-1}, \quad \mathbf{B}' = -\mathbf{A}^{-1}\mathbf{B}\mathbf{D}', \quad \mathbf{C}' = -\mathbf{D}'\mathbf{B}\mathbf{A}^{-1}, \quad \mathbf{D}' = [\mathbf{D} - \mathbf{B}\mathbf{A}^{-1}\mathbf{B}]^{-1}, \quad (22)$$

$$\mathbf{f}' = -\mathbf{B}'\mathbf{g} - \mathbf{A}'\mathbf{f}, \quad \mathbf{g}' = -\mathbf{C}'\mathbf{f} - \mathbf{D}'\mathbf{g}. \quad (23)$$

Arrays  $\mathbf{f}'$  and  $\mathbf{g}'$  are overall eigen-strain and curvature.

In general, six transformation stress components can occur in a lamina. However, only the in-plane components  $\hat{\boldsymbol{\lambda}}_i = [\lambda_{i1}, \lambda_{i2}, \lambda_{i3}]$  cause in-plane stresses in the perfectly bonded plies. The out-of-plane transformation strains caused in the plies can be accommodated without introducing additional in-plane stresses. The lamina stresses caused by mechanical loads,  $\mathcal{N}$  and  $\mathcal{M}$ , together with the lamina transformation stresses can then be written as the sum of the individual contributions,

$$\hat{\boldsymbol{\sigma}}_i = \mathbf{P}_i\mathcal{N} + \mathbf{Q}_i\mathcal{M} + \sum_{j=1}^n \mathbf{U}_{ij}\hat{\boldsymbol{\lambda}}_j, \quad i = 1, 2, \dots, n, \quad (24)$$

Matrices  $\mathbf{P}_i$  and  $\mathbf{Q}_i$ ,  $i, j = 1, 2, \dots, n$ , are stress distribution factors, and  $\mathbf{U}_{ij}$  is stress transformation influence function.

In the absence of ply eigenstresses, the distribution factors are found by averaging the in-plane strain of Eq. (17) over the ply thickness, utilizing (21), and substituting the result in Eq. (11). The result is

$$\mathbf{P}_i = \hat{\mathbf{L}}_i(\mathbf{A}' + z_i\mathbf{C}'), \quad \mathbf{Q}_i = \hat{\mathbf{L}}_i(\mathbf{B}' + z_i\mathbf{D}'). \quad (25)$$

The influence function  $\mathbf{U}_{ij}$  can be recovered from the same procedure if ply eigenstresses are present. Alternately, they can be found by first introducing an eigenstress  $\hat{\boldsymbol{\lambda}}_j$  in ply 'j' of a laminate, which is otherwise free from stresses. The equilibrating overall forces and bending moments are then found from Eqs. (1) and (2) as

$$\mathcal{N} = \sum_{i=1}^n \left( \int_{z_i-t_i/2}^{z_i+t_i/2} \hat{\boldsymbol{\sigma}}(z) dz \right) = t_j \hat{\boldsymbol{\lambda}}_j, \quad \mathcal{M} = \sum_{i=1}^n \left( \int_{z_i-t_i/2}^{z_i+t_i/2} z \hat{\boldsymbol{\sigma}}(z) dz \right) = (t_j z_j) \hat{\boldsymbol{\lambda}}_j. \quad (26)$$

Finally, the forces and bending moments of Eq. (26) are removed and the ply stresses due to  $\hat{\boldsymbol{\lambda}}_j$  are computed as the sum of the contributions found in this loading sequence. Transformation influence functions of a ply are then found as

$$U_{ij} = \delta_{ij} \mathbf{I} - t_j \mathbf{P}_i - (t_j z_j) \mathbf{Q}_i. \quad (27)$$

where  $\delta_{ij}$  is the Kronecker's tensor, and  $\mathbf{I}$  is identity matrix.

Certain identities can be recovered for the stress distribution factors when, in the absence of eigenstresses, Eq. (24) is utilized in the equilibrium equations, Eqs. (1) and (2), and the stress is averaged over the ply thickness. The result is

$$\sum_{i=1}^n t_i \mathbf{P}_i = \mathbf{I}, \quad \sum_{i=1}^n t_i \mathbf{Q}_i = \mathbf{0}, \quad \sum_{i=1}^n (t_i z_i) \mathbf{P}_i = \mathbf{0}, \quad \sum_{i=1}^n (t_i z_i) \mathbf{Q}_i = \mathbf{I}. \quad (28)$$

Since stress averages are used in deriving Eqs. (28), these identities will be satisfied, within a small tolerance, if the plies are fairly thin. In this case, subdividing the individual laminas into several layers results in a better resolution of the stress distribution, and hence accurate prediction of the overall response. This, in particular, is important when curvature of the laminate does not vanish and ply failure is of interest since the associated criteria are based on stress averages.

## V. Transformation Field Analysis

The schematic of Fig. 2 shows the relationships derived in Sections III and IV between stresses in the fiber and matrix of a lamina, the individual plies, and the laminate. It illustrates how the TFA approach propagates the effects of local phenomena, quantified by eigenstresses,  $\lambda_f, \lambda_m$  in the fiber and matrix, and/or  $\hat{\boldsymbol{\lambda}}_i$  in the individual plies, across multiple length scales. In preparation for applying the method to damage, we derive here equations for ply and phase stresses in terms of the applied loads and the eigenstresses.

Referring to material principal axes of a ply, the lamina overall stresses caused by the applied loads  $\mathcal{N}$  and  $\mathcal{M}$ , and ply eigenstresses  $\hat{\lambda}_j$ ,  $j=1,2,\dots,n$ , can be found from Eq. (24) and the stress transformation rules of Eqs. (12) and (13). The result is

$$\hat{\sigma}_i = \mathbf{R}_i \left( \mathbf{P}_i \mathcal{N} + \mathbf{Q}_i \mathcal{M} + \sum_{j=1}^n \mathbf{U}_{ij} \mathbf{N}_j^T \hat{\lambda}_j \right), \quad i=1,2,\dots,n. \quad (29)$$

In treating failure in fibrous plies (Section VI), a mixed formulation is used in which axial, normal eigenstresses,  $\lambda_{11}^f$ ,  $\lambda_{11}^m$ , are introduced in the fiber and matrix, while transverse normal and longitudinal, in-plane shear eigenstresses are introduced in the ply. Denoting the latter by  $\bar{\lambda}_{22}^*$  and  $\bar{\lambda}_{12}^*$  and utilizing Eqs. (8) and (16) to determine the contribution of the axial eigenstress in the phases to the ply eigenstress, Eq. (29) is rewritten as

$$\hat{\sigma}_i = \mathbf{R}_i (\mathbf{P}_i \mathcal{N} + \mathbf{Q}_i \mathcal{M}) + \mathbf{R}_i \sum_{j=1}^N \mathbf{U}_{ij} \mathbf{N}_j^T \left\{ \begin{array}{l} v_f A_{11}^{(f)} \lambda_{11}^f + v_m A_{11}^{(m)} \lambda_{11}^m \\ \bar{\lambda}_{22}^* + v_f A_{12}^{(f)} \lambda_{11}^f + v_m A_{12}^{(m)} \lambda_{11}^m \\ \bar{\lambda}_{12}^* + v_f A_{16}^{(f)} \lambda_{11}^f + v_m A_{16}^{(m)} \lambda_{11}^m \end{array} \right\}^{(j)}, \quad i=1,2,\dots,n, \quad (30)$$

where  $\mathbf{A}_r \equiv A_{kl}^{(r)}$  is strain concentration matrix of phase ‘ $r$ ’. The first term in Eq. (30) provides the ply stress caused by the applied loads. The second term indicates the effect of directly applied ply eigenstresses as well as those caused by phase eigenstresses due to imposition of equal in-plane strain condition on the fully bonded plies.

The phase stresses are given by Eq. (6)<sub>2</sub> in terms of the full stress vector of the ply in local coordinates and the phase eigenstresses. Again considering only axial, normal eigenstresses in the matrix and fiber, and reducing the full stress vectors to their in-plane counterparts using Eq. (16), the phase stresses in ply ‘ $i$ ’ can be written as

$$\sigma_r^{(i)} = \mathbf{B}_r^{(i)} \hat{\mathbf{I}} \hat{\sigma}_i + \lambda_{11}^f \mathbf{f}_1^{(rf)} + \lambda_{11}^m \mathbf{f}_1^{(rm)}, \quad r=f,m, \quad (31)$$

where  $\mathbf{F}_{rs} = (\mathbf{f}_1^{(rs)}, \dots, \mathbf{f}_6^{(rs)})$  is stress transformation influence function. Substituting for the ply stresses from Eq. (30), we find

$$\sigma_r^{(i)} = \mathbf{B}_r^{(i)} \hat{\mathbf{I}} \mathbf{R}_i (\mathbf{P}_i \mathcal{N} + \mathbf{Q}_i \mathcal{M}) + \mathbf{B}_r^{(i)} \hat{\mathbf{I}} \mathbf{R}_i \sum_{j=1}^N \mathbf{U}_{ij} \mathbf{N}_j^T \left\{ \begin{array}{l} v_f A_{11}^{(f)} \lambda_{11}^f + v_m A_{11}^{(m)} \lambda_{11}^m \\ \bar{\lambda}_{22}^* + v_f A_{12}^{(f)} \lambda_{11}^f + v_m A_{12}^{(m)} \lambda_{11}^m \\ \bar{\lambda}_{12}^* + v_f A_{16}^{(f)} \lambda_{11}^f + v_m A_{16}^{(m)} \lambda_{11}^m \end{array} \right\}^{(j)}, \quad (32)$$

$$+ (\lambda_{11}^f \mathbf{f}_1^{(rf)} + \lambda_{11}^m \mathbf{f}_1^{(rm)})^{(i)}, \quad r=f,m.$$

The first term in Eq. (32) provides the local stress caused by the applied loads. The last two terms represent the local stress caused in the fiber and matrix of lamina ‘i’ by eigenstresses found in the plies as well as those found in their fiber and matrix phases. These represent two effects, one due to the constraints introduced by the assumption of fully bonded fiber and matrix in lamina ‘i’, and one due to the assumption of fully bonded laminas which forces the in-plane strains of the plies to be equal.

In utilizing Eq. (30) and/or Eq. (32) to model local damage in fibrous laminates, the scheme developed by Bahei-El-Din et al.<sup>10</sup> is applied. It centers on finding an auxiliary transformation stress field in the plies and/or their fiber and matrix phases such that the magnitude of the corresponding net stress components, which violate the underlying failure criteria are zero. Hence, brittle failure is implied and is expected to prevail for example in polymer matrix composites. This is achieved by first finding the stresses in an undamaged laminate subjected to a given overall load using the first term of Eqs. (30) and (32). Next, the relevant failure criteria are examined for all plies, and the violating stress components are identified. Finally, setting the violating stress components to zero in the left hand side of Eqs. (30) and (32), the eigenstresses can be computed by inverting the resulting algebraic equations. Since the computed eigenstress field will alter the stresses in the undamaged plies, the process is repeated until no further damage is found under the applied overall loads.

The response under a given overall stress path is found by updating the overall load by small increments and repeating the transformation field analysis under the entire applied load. Local stress components marked for violating the failure criteria in previous loading steps are included in the process for determining the auxiliary eigenstress field such that the history of previous damage is accounted for.

## VI. Failure Criteria

Two classes of failure criteria are considered for a fibrous lamina and their effect on the predicted overall response of laminates is quantified in the next section, one is macromechanical and one is micromechanical. In the macromechanical approach, failure is examined in terms of the overall, in-plane stress of a ply,  $\hat{\sigma}$ , referred to the material principal coordinates. In this case failure is indicated when the stress state is contained by a failure envelope,

$$f(\hat{\sigma}) = 0. \quad (33)$$

For example Eq. (33) can be represented by the failure envelope proposed by Tsai and Wu<sup>23</sup>. If the stresses  $\hat{\sigma} = (\bar{\sigma}_{11}, \bar{\sigma}_{22}, \bar{\sigma}_{12})$  caused in an undamaged ply ‘*i*’ by the applied loads satisfy Eq. (33), we seek eigenstresses  $\hat{\lambda}_i^* = (\bar{\lambda}_{11}^*, \bar{\lambda}_{22}^*, \bar{\lambda}_{12}^*)$  such that  $\hat{\sigma} = \theta$ . Solution of this problem is obtained from Eq. (30). Hence, this approach is equivalent to the ply discount method applied by O’Brien<sup>24</sup>.

In the micromechanical approach, the onset of failure is determined based on the stress state found in the fiber and matrix. In the present work, averaging models are utilized to evaluate the local stresses. Hence, the average phase stresses in the undamaged state are given by the first term of Eq. (32) where, under the laminate geometry considered here, four stress components may in general exist,  $\sigma_{11}^{(r)}, \sigma_{22}^{(r)}, \sigma_{33}^{(r)}, \sigma_{12}^{(r)}$ ,  $r = f, m$ .

Failure under axial stress  $\sigma_{11}^{(r)}$  occurs when the stress magnitude equals the ultimate strength. To account for different strength magnitudes under tensile and compressive stresses, the respective values are denoted by  $\sigma_{uT}^{(r)}$  and  $\sigma_{uC}^{(r)}$ , and the failure criterion is written as

$$\sigma_{11}^{(r)} = \sigma_{uT}^{(r)} \quad \text{if } \sigma_{11}^{(r)} > 0, \quad \sigma_{11}^{(r)} = \sigma_{uC}^{(r)} \quad \text{if } \sigma_{11}^{(r)} < 0, \quad r = f, m, \quad (34)$$

and the eigenstress sought from Eq. (32) to remove the axial stress in the phase is  $\lambda_{11}^i$ . It is assumed in the subsequent results, however, that the phase strength magnitudes under axial tension and compression stresses are equal.

Under transverse normal stresses, matrix failure may occur by slip on planes parallel to the fiber when the resolved shear stress exceeds the ultimate shear strength of the matrix. The slip direction in this case is transverse to the fibers. Considering frictional slip, failure criterion of the matrix in this case can be written as,

$$\frac{1}{2} |\sigma_{33}^m - \sigma_{22}^m| + \frac{1}{2} \eta_T \langle \sigma_{33}^m + \sigma_{22}^m \rangle = \tau_u^m, \quad (35)$$

where  $\eta_T$  is coefficient of friction for matrix slip in the transverse direction,  $\langle x \rangle = x$  if  $x < 0$ , and  $\langle x \rangle = 0$  if  $x \geq 0$ .

We note that consideration of friction provides a mean for distinction between tensile and compressive failure. An entirely different failure mode which may occur in the matrix is transverse cracking under tensile stresses, or compressive failure. The limiting conditions in this case are,

$$\sigma_{22}^m = \sigma_{uT}^m \quad \text{if } \sigma_{22}^m > 0, \quad \sigma_{22}^m = \sigma_{uC}^m \quad \text{if } \sigma_{22}^m < 0. \quad (36)$$

Since inability of the matrix to transmit transverse stress implies failure of the ply under transverse loading, we require  $\bar{\sigma}_{22}$  in Eq. (30) to vanish by introducing eigenstress  $\bar{\lambda}_{22}^*$  if either Eq. (35) and/or Eq. (36) are satisfied.

Under longitudinal shear, matrix failure may occur by slip in the longitudinal direction on planes parallel to the fiber. Considering again frictional slip, the onset of failure is written as

$$\sigma_{12}^m + \eta_L \langle \sigma_{22}^m \rangle = \tau_u^m, \quad (37)$$

where  $\eta_L$  is coefficient of friction for matrix slip in the longitudinal direction. Here too, this failure mode implies inability of the ply to support shear loading, and as such we require  $\bar{\sigma}_{12}$  in Eq. (30) to vanish by introducing eigenstress  $\bar{\lambda}_{12}^*$ .

Since ply strength is matrix-dominated under transverse loads and shear stresses, no failure criteria are specified under these stress components for the fiber. We note however that these stresses will vanish in the fiber when the matrix fails and the ply stresses accordingly vanish. This of course is a consequence of the two-phase, averaging models of fibrous composites that are utilized here.

## VII. Results

Mechanical behavior of fibrous laminates tested by Soden et al.<sup>25,26</sup> was predicted with the multiscale TFA model described above. Two composite systems are considered; AS4 carbon/epoxy and Silenka E-glass/epoxy. Mechanical properties of the fibers and two types of epoxy matrices are given in Tables 1 and 2. Mechanical properties of the unidirectional composites are given in Table 3 and their ultimate strength magnitudes are given in Table 4. Also shown in Table 3 are elastic moduli of the unidirectional composites as predicted by the Mori-Tanaka averaging model<sup>27</sup>. We note that certain strength properties of the DY063 epoxy listed in Table 2, which are not available from experiments have been back calculated by matching the overall strength given in Table 4 and using the failure criteria of Section VI. For example, the matrix ultimate strength under tension and compression are computed from their overall counterparts under transverse loading of a unidirectional lamina by utilizing Eq. (36). For E-glass/DY063-epoxy, the overall strength measured under uniaxial transverse tensile load is  $\bar{\sigma}_{22} = 40$  MPa (Table 4), and the matrix stress concentration factor, Eq. (6)<sub>2</sub>, given by the Mori-Tanaka model<sup>27</sup> under this load is  $B_{22}^m = 0.793$ . Hence, the tensile strength of the matrix is computed as  $\sigma_{uT}^m = B_{22}^m \bar{\sigma}_{22} = 31.72$  MPa (Table 2). Using

the same concentration factor and the measured overall compressive strength under transverse load of 145 MPa provides the ultimate compressive strength of the matrix as 115 MPa.

Under longitudinal shear, the E-glass/DY063-epoxy composite fails at  $\bar{\sigma}_{12} = 73$  MPa (Table 4). With a Mori-Tanaka stress concentration factor  $B_{12}^m = 0.635$ , the matrix ultimate strength in shear is computed as 46.35 MPa (Table 2). The longitudinal coefficient of friction  $\eta_L$  is determined from a combined transverse compression/longitudinal shear test. From Table 4, we find  $\bar{\sigma}_{22} = -70.5$  MPa and  $\bar{\sigma}_{12} = 96.6$  MPa. With these overall strength magnitudes, and the above stress concentration factors under transverse normal and longitudinal shear stresses,  $B_{22}^m$  and  $B_{12}^m$ , Eq. (37) provides  $\eta_L = 0.268$  (Table 2).

Figures 3 and 4 compare the predicted and measured stress-strain responses for two laminates,  $(90/\pm 45/0)_s$  AS4-carbon/3501-6-epoxy, and  $(\pm 45)_s$  E-glass/DY063-epoxy. Figure 5 compares failure envelopes of the quasi-isotropic laminate in the biaxial stress plane. Close agreement between the experimental measurements and the micromechanics-based TFA predictions are seen in all figures, while prediction of the ply-discount approach underestimates the overall strength by a substantial margin. The onset of damage modes predicted by the TFA is indicated by the numbered circles in Figs. 3 and 4 and the table insert. Damage in the carbon/epoxy quasi-isotropic laminate, which is primarily loaded along the  $90^\circ$  plies, is initiated in the matrix of the  $0^\circ$  ply in the form of longitudinal splitting due to exceeding the normal strength, Fig. 3. This is followed by shear failure of the matrix in the  $45^\circ$  plies. Ultimate failure of the laminate is triggered by breakage of the fibers in the  $90^\circ$  plies.

Damage in the E-glass/epoxy,  $(\pm 45)_s$  laminate is also initiated by longitudinal splitting of the matrix due to exceeding its normal strength in the transverse direction in all plies, followed by failure on matrix transverse planes, Fig. 4. Ultimate failure of the laminate is caused by shear failure of the matrix in all plies. We note that the theoretical predictions provide equal overall normal strains as expected under the applied load. On the other hand unequal strain magnitudes are found in the experiment, which is indicative of possible misalignment of the fiber orientations.

Finally, it is seen from Fig. 5 that the strength magnitudes which are measured experimentally<sup>26</sup> for the carbon/epoxy, quasi-isotropic laminate scatter around the predicted envelope.

## VIII. Closure

Modeling progressive damage in fibrous laminates is essential for reliable predictions of their behavior and ultimate loads. The transformation field analysis described in this paper provides a rigorous approach for evaluation of the effect of failure initiated in the constituents on the local fields and overall response of laminates subjected to membrane and bending loads. Both the micromechanical model employed to represent the individual fibrous laminae and the local failure models affect the predictions. In the present work, averaging models of fibrous composites have been utilized. More refined, unit cell models are expected to provide a more gradual progression of damage in contrast to the abrupt changes in the overall strains seen in damage predictions based on averaging models. Computational cost of the former models however is expected to be rather high particularly in uncertainty designs of composite panels<sup>28</sup>.

## Acknowledgments

This work was supported by a grant from the Air Force Office of Scientific Research, Directorate of Aerospace and Materials Sciences. Dr. B.L. Lee, Program Manager, Mechanics of Materials and Devices, served as project monitor. This work was performed at Rensselaer Polytechnic Institute while YAB was a visiting professor.

## References

- <sup>1</sup> Bahei-El-Din Y.A., Mullur, A. A., Hajela, P., Peters, J., and Dvorak, G.J., “Nondeterministic Modeling of Progressive Failure in Laminated Composites,” *2nd Multidisciplinary Design Optimization Specialist Conference*, AIAA-2006-2144, Newport, RI, May 2006.
- <sup>2</sup> Khire, R., Bahei-El-Din, Y.A., and Hajela, P., “Uncertainty Propagation in Multiscale Transformation Field Analysis of Laminated Composites,” *3rd AIAA Multidisciplinary Design Optimization Specialist Conference*, Honolulu, Hawaii, April 2007.
- <sup>3</sup> Dvorak, G. J., “Transformation Field Analysis of Inelastic Composite Materials,” *Proceedings of the Royal Society London*, Vol. A437, 1992, pp. 311–327.
- <sup>4</sup> Dvorak, G.J. and Benveniste, Y., “On Transformation Strains and Uniform Fields in Multiphase Elastic Media,” *Proceedings of the Royal Society London*, Vol. A437, 1992, pp. 291–310.
- <sup>5</sup> Dvorak, G.J., Bahei-El-Din, Y.A., and Wafa, A.M., “Implementation of the Transformation Field Analysis for Inelastic Composite Materials,” *Computational Mechanics*, Vol. 14, 1994, pp. 201-228.
- <sup>6</sup> Dvorak, G.J. and Zhang, J., “Transformation field analysis of damage evolution in composite materials,” *Journal of the Mechanics and Physics of Solids*, Vol. 49, 2001, pp. 2517-2541.

- <sup>7</sup> Dvorak, G.J. and Sejnoha, M., 1995, "Initial Failure Maps of Fibrous CMC Laminates," *Journal of the American Ceramic Society*, Vol. 78, 1995, pp. 205-210.
- <sup>8</sup> Bahei-El-Din, Y.A., "Finite Element Analysis of Viscoplastic Composite Materials and Structures," *Mechanics of Composite Materials and Structures*, Vol. 3, 1996, pp. 1-28.
- <sup>9</sup> Bahei-El-Din, Y.A. and Botrous, A.G., "Analysis of Progressive Fiber Debonding in Elastic Laminates," *International Journal of Solids and Structures*, Vol. 40, 2003, pp. 7035-7053.
- <sup>10</sup> Bahei-El-Din, Y.A., Rajendran, A.M., and Zikry, M.A., "A Micromechanical Model for Damage Progression in Woven Composite Systems," *International Journal of Solids and Structures*, Vol. 41, 2004, pp. 2307-2330.
- <sup>11</sup> Fish, J., Yu, Q., and Shek, K.L., "Computational Damage Mechanics for Composite Materials Based on Mathematical Homogenization," *International Journal of Numerical Methods in Engineering*, Vol. 45, 1999, pp. 1657-1679.
- <sup>12</sup> Chaboche, J.L., Kruch, S., Maire, J.F., and Pottier, T., "Towards a Micromechanics Based Inelastic and Damage Modeling of Composites," *International journal of Plasticity*, Vol. 17, 2001, pp. 411-439.
- <sup>13</sup> Michel, J.C. and Suquet, P., "Computational Analysis of Nonlinear Composite Structures Using the Nonuniform Transformation Field Analysis," *Computer Methods in Applied Mechanics and Engineering*, Vol. 193, 2004, pp. 5477-5502.
- <sup>14</sup> Oskay, C. and Fish, J., "Eigendefor-mation-Based Reduced Order Homogenization for Failure Analysis of Heterogeneous Materials," *Computer Methods in Applied Mechanics and Engineering*, Vol. 196, 2007, pp. 1216-1243.
- <sup>15</sup> Bahei-El-Din Y.A. and Dvorak, G.J., "Micromechanics of Inelastic Composite Materials," *Comprehensive Composite Materials*, A. Kelly and C. Zweben, Editors-in-Chief, Chapter 15 in Volume 1: General Theory of Composites, edited by T.-W. Chou, Elsevier Science B.V., Amsterdam, 2000.
- <sup>16</sup> Chuang, S.-N., "Probabilistic Analysis in Unidirectional Fiber-Reinforced Composite Material Design Screening," SAMPE, San Diego, CA, November 2004.
- <sup>17</sup> Hill, R., "Elastic Properties of Reinforced Solids: Some Theoretical Principles," *Journal of the Mechanics and Physics of Solids*, Vol. 11, 1963, pp. 357–372.
- <sup>18</sup> Hill, R., "A Self-consistent Mechanics of Composite Materials," *Journal of the Mechanics and Physics of Solids*, Vol. 13, 1965, pp. 213–222.
- <sup>19</sup> Dvorak, G.J., "Plasticity Theories for Fibrous Composite Materials," *Metal Matrix Composites, Mechanisms and Properties*, Vol. 2, edited by R.K. Everett and R.J. Arsenault, Academic Press, Boston, 1991, pp. 1–77.
- <sup>20</sup> Levin, V.M., "Thermal Expansion Coefficients of Heterogeneous Materials," *Mechanics of Solids*, Vol. 11, 1967, pp. 58–61.
- <sup>21</sup> Bahei-El-Din, Y.A., "Uniform Fields, Yielding, and Thermal Hardening in Fibrous Composite Laminates," *International Journal of Plasticity*, Vol. 8, 1992, pp. 867–892.

<sup>22</sup>Hill, R., “Theory of Mechanical Properties of Fiber-Strengthened Materials: I. Elastic Behaviour,” *Journal of the Mechanics and Physics of Solids*, Vol. 12, 1964, pp. 199–212.

<sup>23</sup>Tsai, S.W. and Wu, E.M., “A General Theory of Strength for Anisotropic Materials,” *Journal of Composite Materials*, Vol. 5, 1971, pp. 58-80.

<sup>24</sup>O'Brien, T.K., “An Evaluation of Stiffness Reduction as a Damage Parameter and Criterion for Fatigue Failure in Composite Materials,” Ph.D. Dissertation, 1978, Virginia Polytechnic Institute and State University, Blacksburg, Virginia.

<sup>25</sup>Soden, P.D., Hinton, M.J., and Kaddour, A.S., “Lamina Properties, Lay-up Configurations and Loading Conditions for a Range of Fibre-Reinforced Composite Laminates,” *Composites Science and Technology*, Vol. 58, 1998, pp. 1011-1022.

<sup>26</sup>Soden, P.D., Hinton, M.J., and Kaddour, A.S., “Biaxial Test Results for Strength and Deformation of a Range of E-Glass and Carbon Fibre Reinforced Composite Laminates: Failure Exercise Benchmark Data,” *Composites Science and Technology*, Vol. 62, 2002, pp. 1489–1514.

<sup>27</sup>Mori, T. and Tanaka, K., “Average Stress in Matrix and Average Elastic energy of Materials with Misfitting Inclusions,” *Acta Metallurgica*, Vol. 21, 1973, pp. 571–574.

<sup>28</sup>Khire, R., Hajela, P. and Bahei-El-Din, Y., “Handling Uncertainty Propagation in Laminated Composites Through Multiscale Modeling of Progressive Failure,” AIAA-2007-1913, Proceedings of the 48th AIAA/ASME/ASCE/ AHS/ASC Structures, Structural Dynamics, and Materials Conference, Honolulu, Hawaii, 23-26 April 2007.

**Table 1 Mechanical properties of fiber<sup>(25)</sup>**

Material	$E_L$ (GPa)	$E_T$ (GPa)	$G_L$ (GPa)	$G_T$ (GPa)	$\nu_L$	$\sigma_u$ (GPa)
AS4 Carbon	225	15	15	7	0.2	3.35
Silenka E-glass	74	74	30.8	30.8	0.2	2.15

**Table 2 Mechanical properties of matrix<sup>(25)</sup>**

Material	$E$ (GPa)	$\nu$	$\sigma_{uT}$ (MPa)	$\sigma_{uC}$ (MPa)	$\tau_u$ (MPa)	$\eta_L$
3501-6 epoxy	4.2 <sup>(25)</sup>	0.34 <sup>(25)</sup>	69 <sup>(25)</sup>	250 <sup>(25)</sup>	50 <sup>(25)</sup>	0.3 <sup>(a)</sup>
DY063 epoxy	3.35 <sup>(25)</sup>	0.35 <sup>(25)</sup>	31.72 <sup>(b)</sup>	115 <sup>(b)</sup>	46.36 <sup>(b)</sup>	0.268 <sup>(b)</sup>

<sup>(a)</sup> Assumed

<sup>(b)</sup> Back calculated using properties of unidirectional composites (Table 4)

**Table 3 Elastic moduli of unidirectional composites**

Fiber	Matrix	$\nu_f$	Method	$E_L$ (GPa)	$E_T$ (GPa)	$G_L$ (GPa)	$\nu_L$	$\nu_T$
AS4	3501-6	0.6	Exp <sup>(25)</sup>	126	11	6.6	0.28	0.4
			M-T <sup>(27)</sup>	136.7	14.774	4.5365	0.24729	0.44594
E-glass	MY750/ HY917/ DY063	0.6	Exp <sup>(25)</sup>	45.6	16.2	5.83	0.278	0.4
			M-T <sup>(27)</sup>	45.763	11.019	4.3173	0.25165	0.44047

**Table 4 Ultimate strength of unidirectional composites<sup>(25,26)</sup>**

E-glass/DY063		AS4/3501-6	
$\bar{\sigma}_{22}$ (MPa)	$\bar{\sigma}_{12}$ (MPa)	$\bar{\sigma}_{22}$ (MPa)	$\bar{\sigma}_{12}$ (MPa)
40	0	48	0
-145	0	-200	0
0	73	0	79
-70.5	96.6	-	-

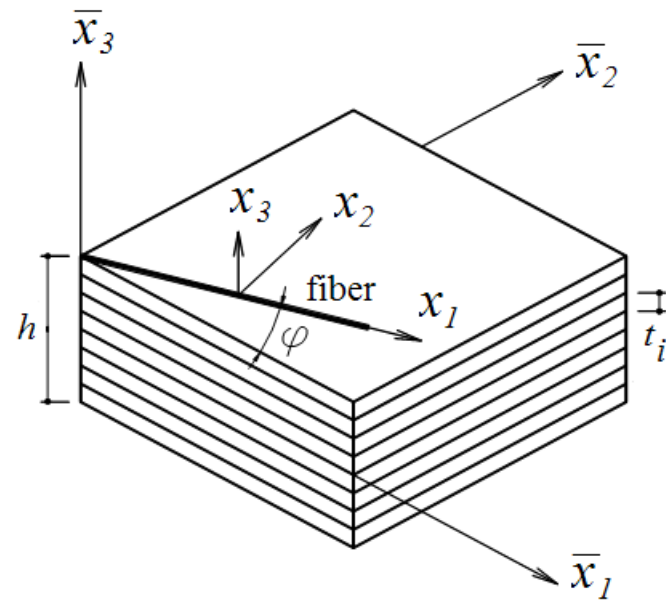


Fig. 1. Geometry of a fibrous laminate.

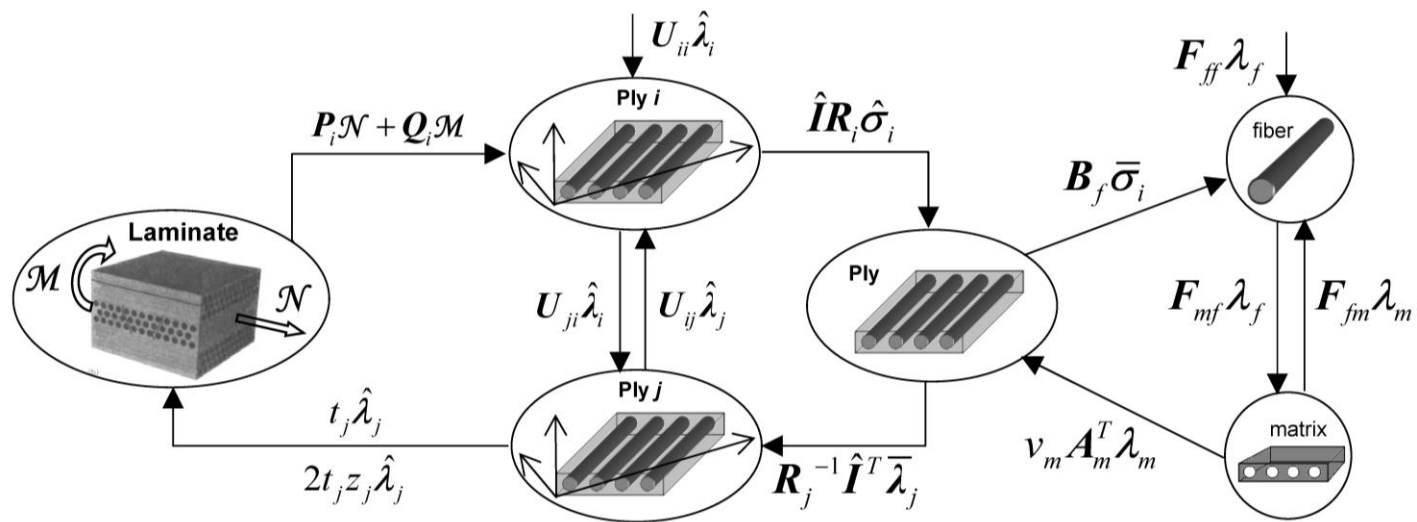


Fig. 2. Schematic of stress flow in multiscale TFA of fibrous laminates subjected to overall membrane forces and bending moments, and local eigenstresses.

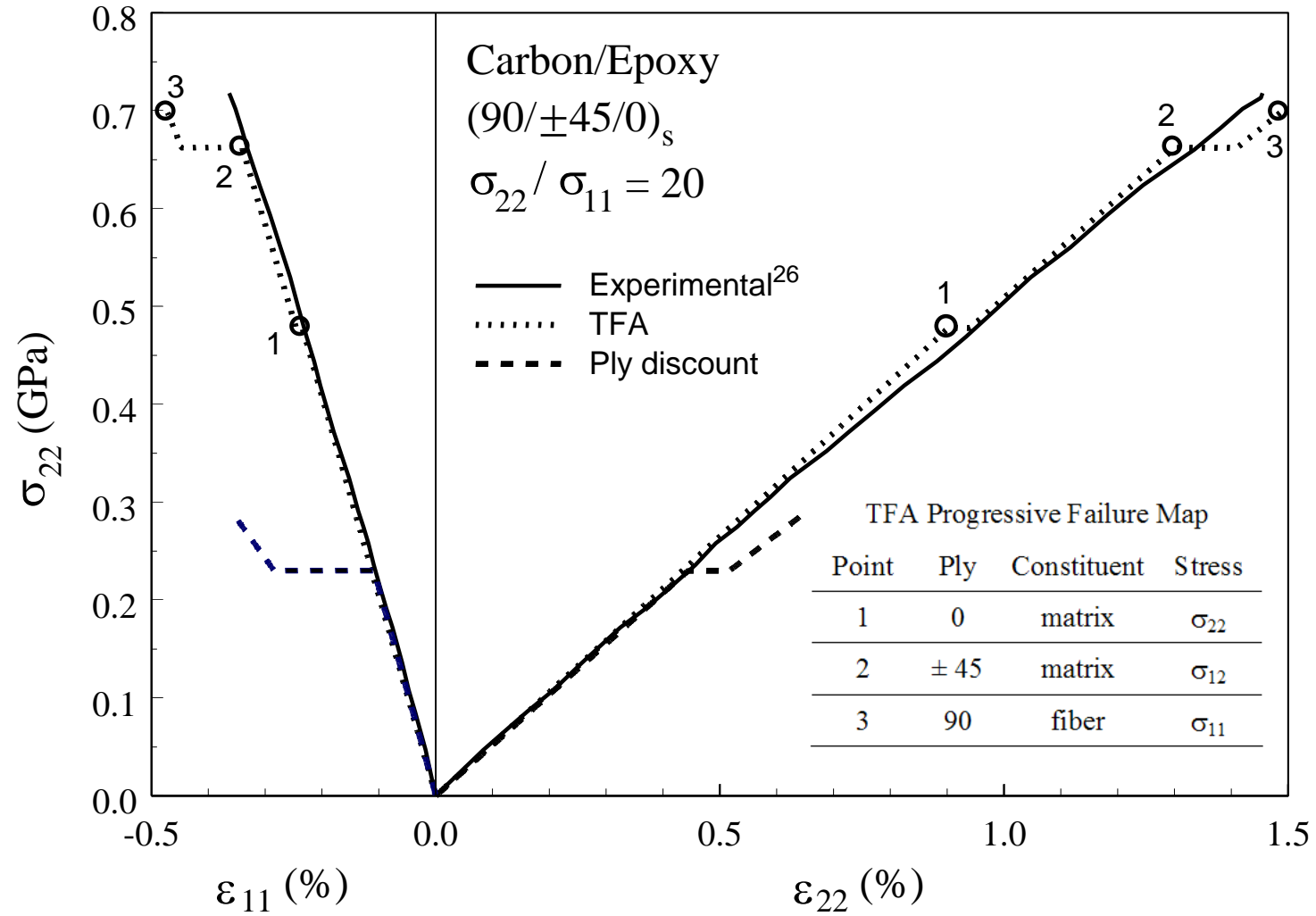


Fig. 3. Comparison of measured and computed stress-strain response of a symmetric, quasi-isotropic, carbon/epoxy laminate.

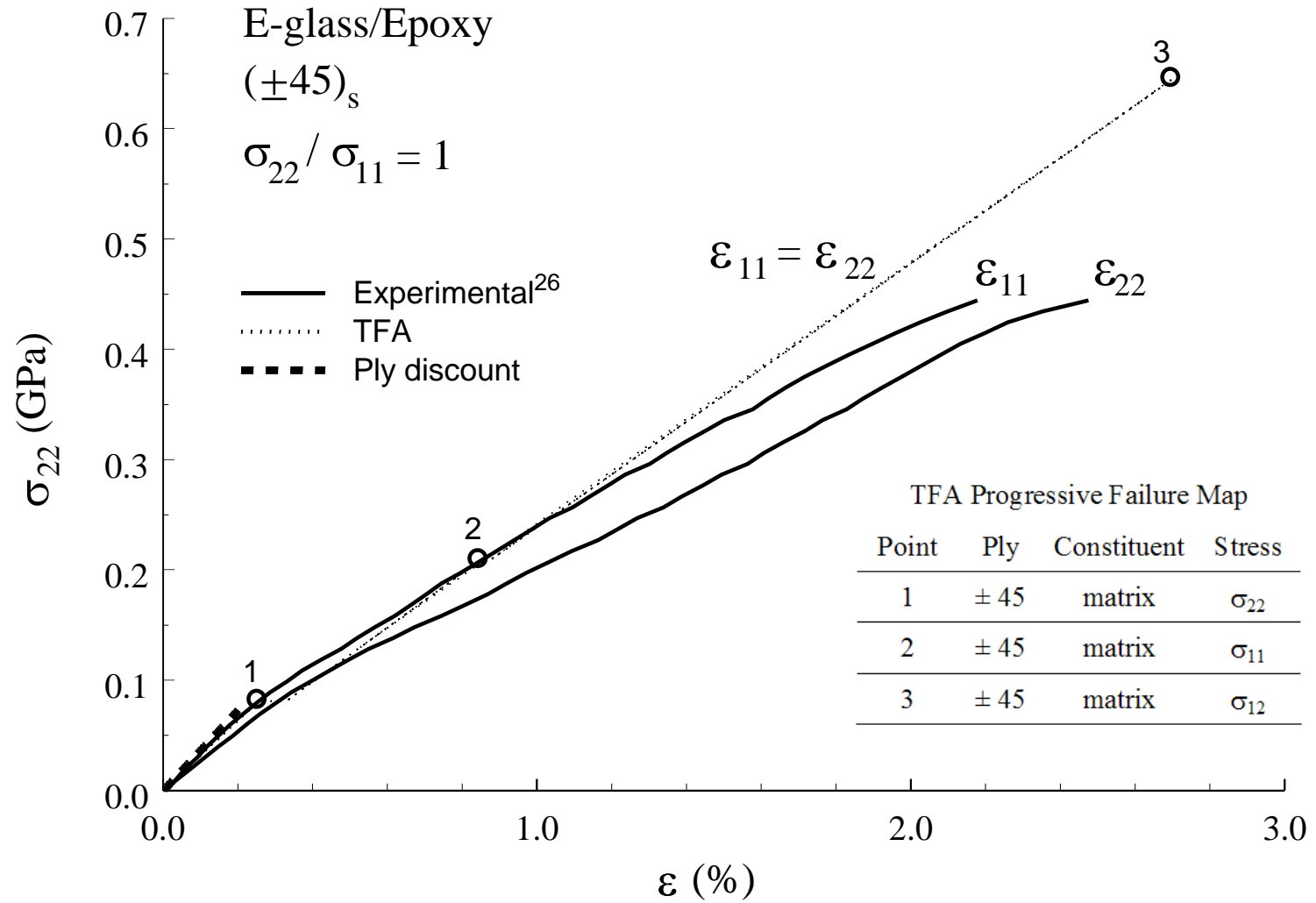


Fig. 4. Comparison of measured and computed stress-strain response of a symmetric  $\pm 45$ , E-glass/epoxy laminate.

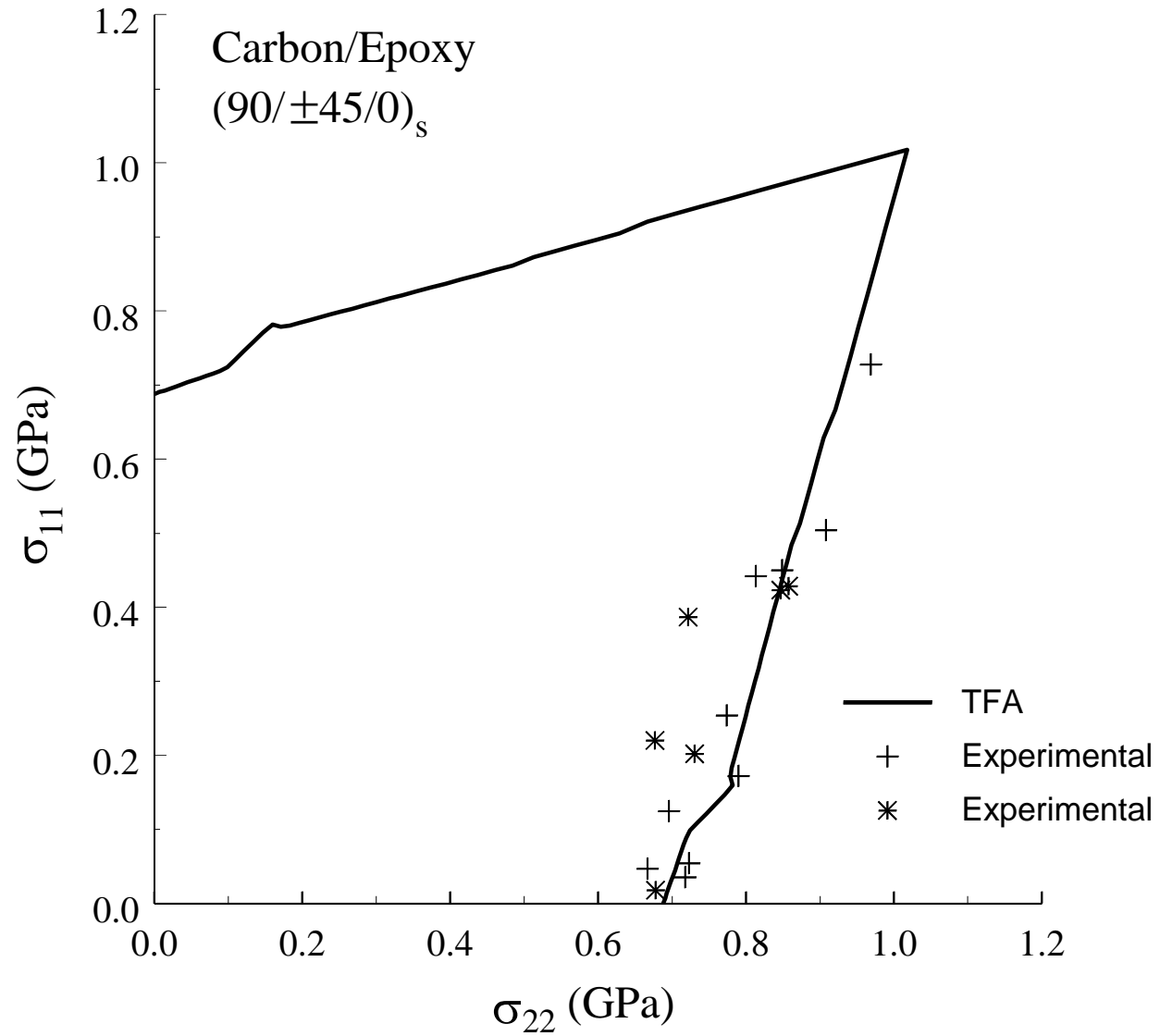


Fig. 5. Comparison of measured and computed failure envelope of a symmetric, quasi-isotropic, carbon/epoxy laminate.